Fermi National Accelerator Laboratory

TM-1579
[SSC-N-598]

Design and Analysis of the SSC Dipole Magnet Suspension System*

T. H. Nicol, R. C. Niemann, and J. D. Gonczy
Fermi National Accelerator Laboratory
P.O. Box 500, Batavia, Illinois

March 1989

* Presented by T. H. Nicol at the 1989 International Industrial Symposium on the Super Collider (IISSC), New Orleans, Louisiana, February 8-10, 1989.

Operated by Universities Research Association, Inc., under contract with the United States Department of Energy

DESIGN AND ANALYSIS OF THE

SSC DIPOLE MAGNET SUSPENSION SYSTEM

T.H. Nicol, R.C. Niemann, J.D. Gonczy

Fermi National Accelerator Laboratory
Batavia, IL

ABSTRACT

The design of the suspension system for Superconducting Super Collider (SSC) dipole magnets has been driven by rigorous thermal and structural requirements. The current system, designed to meet those requirements, represents a significant departure from previous superconducting magnet suspension system designs. This paper will present a summary of the design and analysis of the vertical and lateral suspension as well as the axial anchor system employed in SSC dipole magnets.

INTRODUCTION

The suspension system in a superconducting magnet performs two functions. First it resists structural loads imposed on the cold mass assembly ensuring stable operation over the course of the magnet's operating life. Second it serves to insulate the cold mass from heat conducted from the environment.

The evolution and selection of the suspension system for SSC dipole magnets has been well documented over the course of the past several years.[1,2] The purpose of this paper is not to reiterate the selection process, but rather to give a detailed accounting of the current design, the analysis used in predicting its performance, and the selection of suspension component materials.

Figure 1 illustrates the major components of the suspension system. The magnet assembly is supported vertically and laterally at five places along its length. To accommodate axial shrinkage during cooldown, the magnet assembly is free to slide axially at all but the center support. The center serves as the anchor position. To distribute any imposed axial load to all five supports, tie bars are used to connect the top of each post to its neighbor(s). That is, any vertical or lateral load applied to the magnet assembly is transmitted directly to the supports. An axial load is transmitted to the center post and in turn to the outboard supports through the tie bars.

Table 1 provides a summary of both the structural and thermal design criteria for the suspension system.[3]

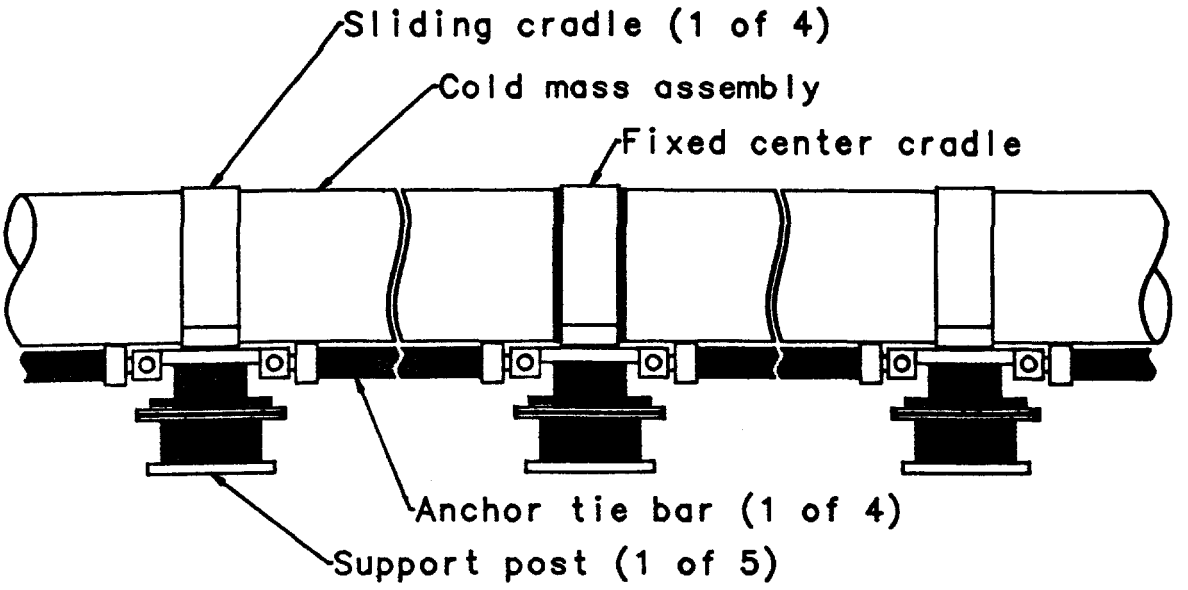

Figure 1. SSC Suspension System Components

SUPPORT POST DESIGN AND ANALYSIS

Figure 2 illustrates a cross section through one of the support posts. Each post assembly consists of inner and outer composite tubes connected by an intermediate stainless steel transition tube. Stainless steel and aluminum discs and rings serve to join the tubes and act as tie points to other cryostat components. The goal of the support post design was to select a geometry and set of materials which resulted in an assembly that satisfied both the structural and thermal design constraints referenced by Table 1.

Structural Analysis

The primary structural loads and directions are shown in Figure 3. F_a denotes an axial load applied to the top of the support post through the anchor attachment point. Axial refers to the long axis of the dipole assembly. F_l and F_v denote lateral and vertical loads respectively and are applied to the post through the cold mass cradle. The lines of action for both pass through the cold mass centerline. Shipping, handling, and seismic loads potentially act in all three directions. Quench loads act as an additional axial load. The weight of the cold mass acts as an additional vertical load although it acts opposite to the direction shown in Figure 3.

Table 1. SSC Dipole Structural and Thermal Load Summary

Shipping and handling loads:	vertical	2.0 G
	lateral	1.0 G
	axial	1.5 G
Seismic load guidelines:	Nuclear Regulatory Guide 1.61 vertical and horizontal spectra scaled by 0.3	
Maximum axial quench load:		25000 lb
Budgeted conduction heat loads per magnet:	80 K	7.20 W
	20 K	0.82 W
	4.5K	0.12 W

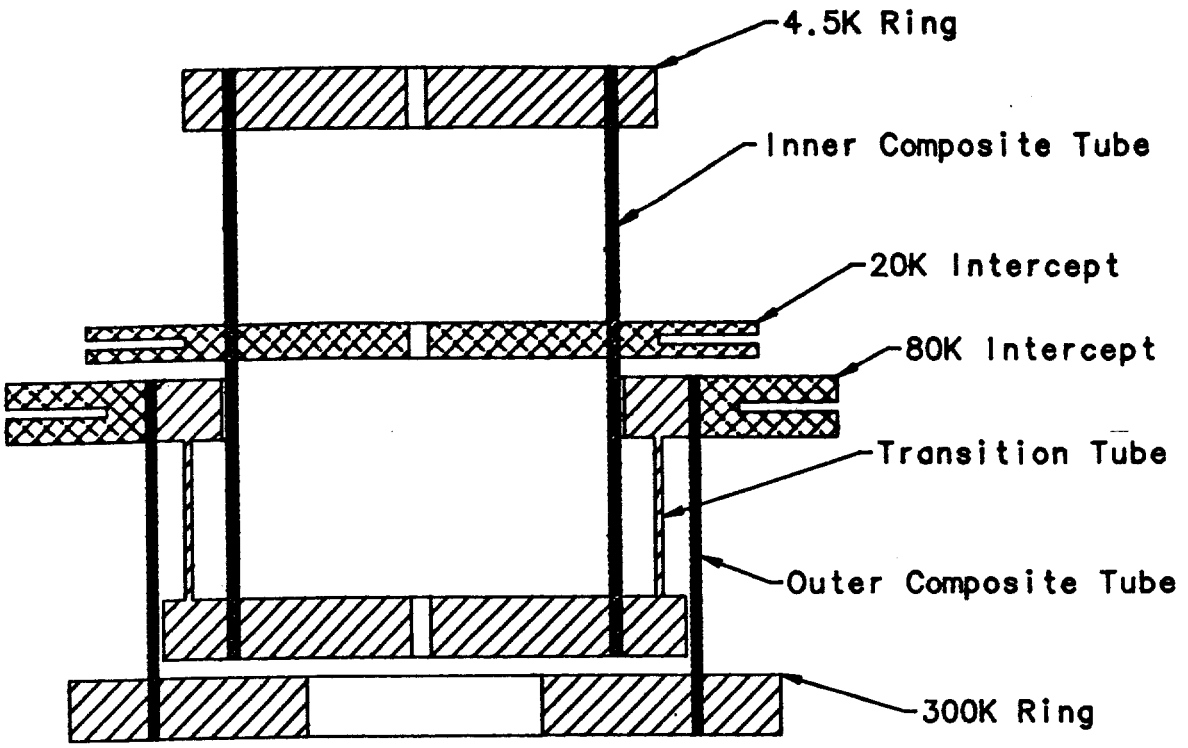

Figure 2. SSC Support Post Cross Section

Experience has shown that the bending loads resulting from the axial and lateral loads produce the highest stresses in the post assembly. Of particular interest are the membrane and shear stresses in the two composite tubes.

Using the notation in Figures 3 and 4 the maximum stresses in tubes 1 (outer) and 2 (inner) due to F_l, F_a, and F_v are

$$\sigma_{il} = \frac{F_l(L_i)d_i}{2I_i} \quad ; \quad \sigma_{ia} = \frac{F_a(L_i - L_3)d_i}{2I_i} \quad ; \quad \sigma_{iv} = \frac{F_v}{A_i} \qquad (1);(2);(3)$$

$$\tau_{il} = \frac{2F_l}{A_i} \quad ; \quad \tau_{ia} = \frac{2F_a}{A_i} \qquad (4);(5)$$

where σ_{il}, σ_{ia}, σ_{iv} = bending stresses resulting from lateral, axial, and vertical loads in tube i

τ_{il}, τ_{ia} = shear stresses resulting from lateral and axial loads in tube i

L_i = L_1 or L_2

The σ_i's are the stresses acting along the axis of each tube. The τ_i's are the shear stresses acting through the respective cross sections. For thin walled tubes there are three values for limiting stresses induced by F_l, F_a, and F_v. They are the ultimate tensile stress, ultimate shear stress, and the stress which causes elastic instability in the tube wall (local buckling). The ultimate tensile and shear stresses are specified to the tube manufacturer and are used to determine the fiber and resin types and the fiber orientation. The stress which causes elastic instability is determined by the composite material properties and the tube geometry. For a tube like those used in SSC supports, elastic instability will occur whenever[4]

$$\sigma_{ci} > \frac{2E_i t_i}{(1.5)\sqrt{3(1-\nu_i^2)}\,d_i} \qquad (6)$$

where σ_{ci} = critical bending stress at the onset of elastic instablility in tube i

E_i = Young's modulus of tube i

t_i = tube thickness of tube i

ν_i = Poisson's ratio of tube i

d_i = diameter of tube i

The overall height and diameter of the support post and the ratios of the various thermal path lengths are determined in large part by the cryostat configuration and the conductive heat load constraints. The design optimization of the complete assembly essentially consists of determining the composite tube materials and wall thicknesses. Equations (1) through (5) are set equal to the ultimate tensile and shear strengths and to the elastic stability constraint represented by equation (6) to determine the optimum value for the wall thickness. Note that although the wall thickness does not appear explicit in any of equations (1) through (5), it is implicit in the expressions for A and I.

As an example, consider the case of some lateral load, F_l acting on a post assembly. Using equations (1), (4), and (6) the optimum geometry would satisfy the more stringent of the following three criteria.

$$\sigma_{il} = \sigma_{ui}$$

$$\tau_{il} = \tau_{ui}$$

$$\sigma_{il} = \sigma_{ci}$$

where σ_{il}, τ_{il}, σ_{ci} = stresses defined above

σ_{ui} = ultimate tensile strength for tube i

τ_{ui} = ultimate shear strength for tube i

In order to satisfy all of the various load cases, a computer program was written to calculate the tube thicknesses required to satisfy the structural requirements given a set of input criteria. The input consists of the structural loads, material properties, and fixed geometric parameters. The output consists of the tube thicknesses which just satisfy the tensile, shear, and critical stresses above, the resulting stresses, and the resulting thermal performance.

Table 2 contains an output listing from the optimization program for an axial load resulting from a magnet quench. Using this set of input parameters, the resulting thicknesses are 0.109 inches for the outer tube and 0.129 inches for the inner. Both tubes are sized based on the ultimate tensile strength (SigU). The resulting maximum stresses are 20000 psi in the outer tube and 30000 psi in the inner. Note that these are exactly equal to the material ultimates (SigU1 and SigU2) when the ultimates are derated by the safety factor (SF) indicating that the solution represents an optimum condition.

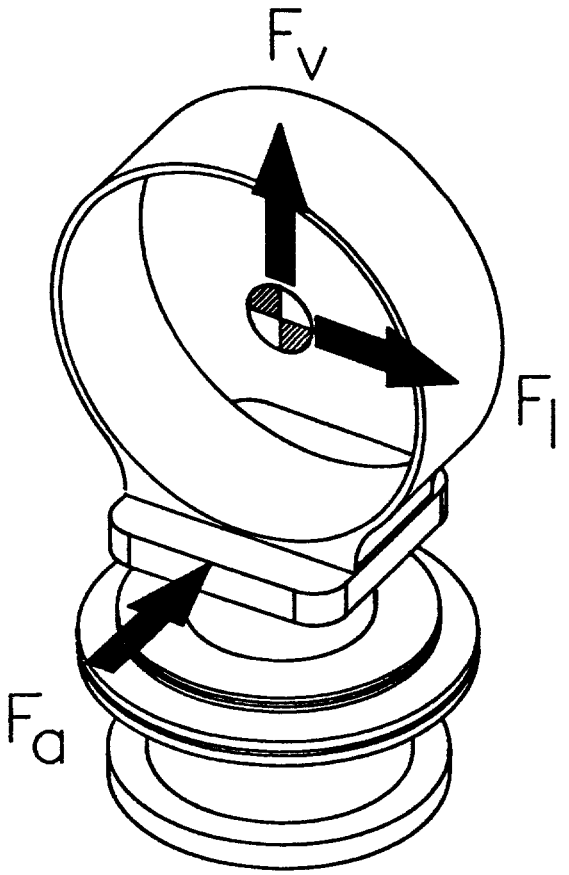

Figure 3. Structural Load and Direction Notation

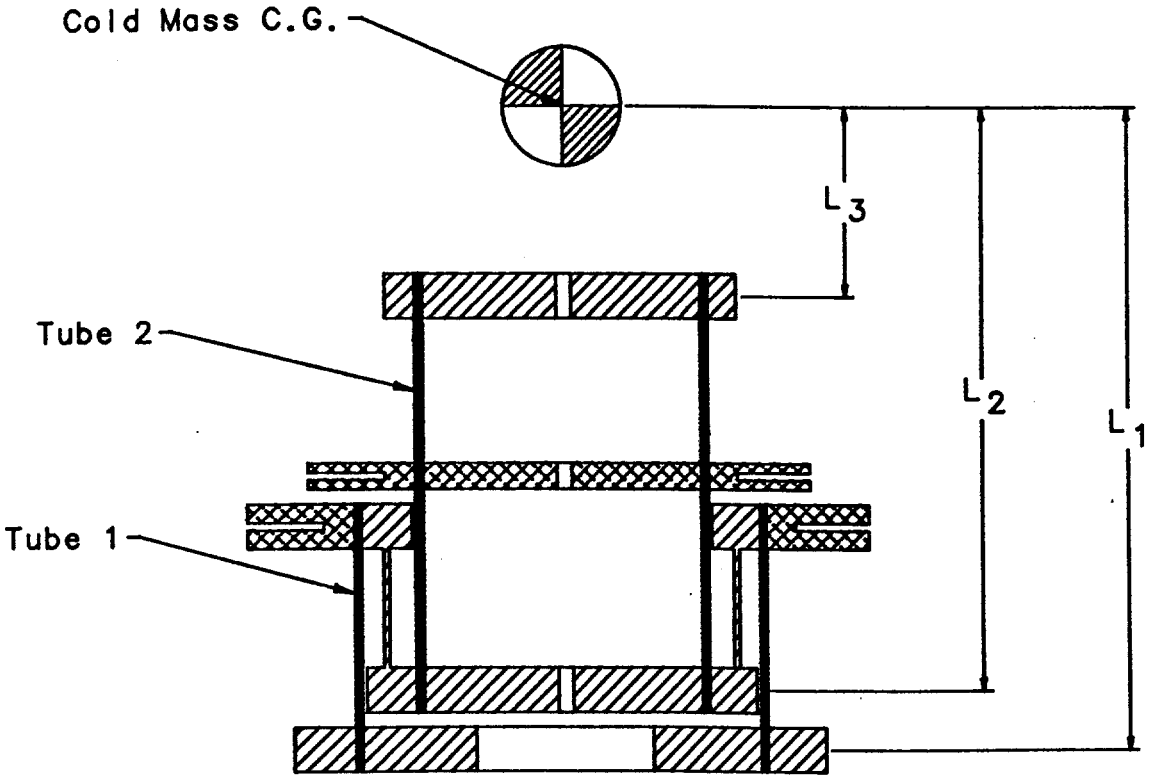

Figure 4. Structural Analysis Notation

Table 2. Summary of Structural Analysis Results

```
*****************************************
*****  Post Optimization...Input  *****
*****************************************

Note.....: Design B - Axial Load
Fg.....(lb):        .0
Fq.....(lb):     8500.0
W......(lb):    -3150.0
SF.............:     2.0
E1.....(psi):    .40E+07
V1.............:     .200
G1.....(psi):    .38E+06
E2.....(psi):    .10E+08
V2.............:     .200
G2.....(psi):    .38E+06
SigU1....(psi):  45000.0
TauU1....(psi):  26000.0
SigU2....(psi):  60000.0
TauU1....(psi):  35000.0
L1.....(in):       14.812
L2.....(in):       13.812
L3.....(in):        6.000
D1.....(in):        7.000
D2.....(in):        5.000
L300_80...(in):     3.000
L80_20....(in):     3.000
L20_Top...(in):     2.375
LTop_45...(in):      .394
ASlide...(in2):      .062
OuterMtl.......:        2  G-11 (WARP)
InnerMtl.......:        3  CARBON FIBER COMPOSITE (UNIAXIAL)
SlideMtl.......:        1  304 STAINLESS STEEL

*****************************************
*****  Resulting Tube Thicknesses  *****
*****************************************

T1 (when sized for SigU)....(in):     .1693
   (when sized for SigEI)...(in):     .0984
   (when sized for TauMx)...(in):     .0782

T2 (when sized for SigU)....(in):     .1287
   (when sized for SigEI)...(in):     .0689
   (when sized for TauMx)...(in):     .0732
```

```
*********************************
*****  Resulting Stresses  *****
*********************************

Sig1 (when sized for SigU)....(psi):   20000.0
     (when sized for SigEI)...(psi):   22099.4
     (when sized for TauMx)...(psi):   27598.7

Sig2 (when sized for SigU)....(psi):   36000.0
     (when sized for SigEI)...(psi):   54121.6
     (when sized for TauMx)...(psi):   51844.3

Tau1 (when sized for SigU)....(psi):    7186.9
     (when sized for SigEI)...(psi):    7964.3
     (when sized for TauMx)...(psi):   10000.0

Tau2 (when sized for SigU)....(psi):    8632.9
     (when sized for SigEI)...(psi):   15938.4
     (when sized for TauMx)...(psi):   15000.0

*************************************************
*****  Resulting Thermal Performance  *****
*************************************************

TTop (when sized for SigU).....(K):    11.2287
     (when sized for SigEI).....(K):    9.4951
     (when sized for TauMx).....(K):    9.6465

Q to 4.5K (when sized for SigU)....(W):     .0153
          (when sized for SigEI)...(W):     .0097
          (when sized for TauMx)...(W):     .0101

Q to 20 K (when sized for SigU)....(W):     .3198
          (when sized for SigEI)...(W):     .1719
          (when sized for TauMx)...(W):     .1827

Q to 80 K (when sized for SigU)....(W):    2.1926
          (when sized for SigEI)...(W):    2.0182
          (when sized for TauMx)...(W):    1.5591
```

Thermal Analysis

In addition to understanding the structural performance of the support posts it is critical that an accurate prediction of the conductive heat load be made to each thermal station. Figure 5 illustrates a thermal model of an SSC support post. Q_{80}, Q_{20}, and $Q_{4.5}$ represent the heat loads to the 80, 20, and 4.5K intercepts respectively and are given by

$$Q_{4.5} = \frac{A_c}{L_c} \int_{4.5}^{T_t} \kappa_i \, dT \tag{7}$$

$$Q_{20} = \frac{A_i}{L_2} \int_{20}^{80} \kappa_o \, dT - Q_{4.5} \tag{8}$$

$$Q_{80} = \frac{A_o}{L_1} \int_{80}^{300} \kappa_o \, dT - Q_{20} - Q_{4.5} \tag{9}$$

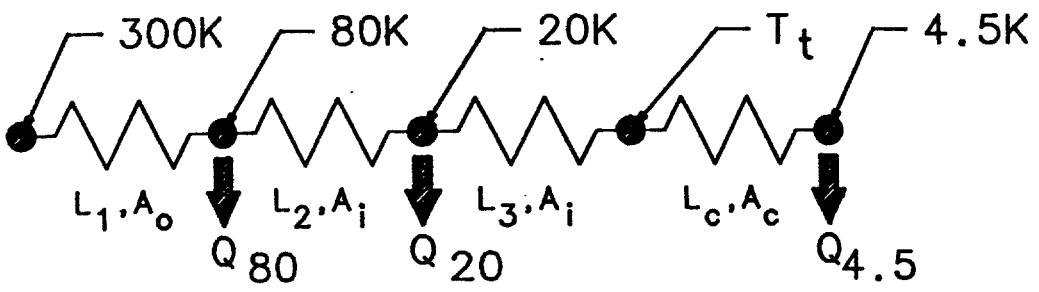

Figure 5. Thermal Analysis Notation

where A_o, A_i = outer and inner tube cross sectional areas
A_c = equivalent cold mass cradle cross sectional area
L_1 = 300K to 80K path length
L_2 = 80K to 20K path length
L_c = equivalent cold mass cradle length
κ_o, κ_i = outer and inner tube thermal conductivities
T_t = temperature at the top of the support post and is found from the steady state solution to

$$\frac{A_i}{L_3}\int_{T_t}^{20}\kappa_i dT = \frac{A_c}{L_c}\int_{4.5}^{T_t}\kappa_c dT \qquad (10)$$

where κ_c = cold mass cradle thermal conductivity
L_3 = 20K intercept to top of support post length

Given a support post geometry and the thermal conductivity integrals for the composite tubes and cold mass cradle, equations (7) through (10) can be solved for the steady state heat loads and the temperature at the top of the post assembly. Again referring to Table 2, the resulting heat loads to 80K, 20K and 4.5K are 2.103, 0.320, and 0.015 W respectively. The equilibrium temperature at the top of the post is 11.2K.

Shrink Fit Joints

Connections between composite tubes and metallic end fittings have historically been made using some form of mechanical fastener or chemical bond. Mechanical fasteners typically introduce unwanted stress concentrations at the joint. Chemical bonds, e.g. epoxy joints, are susceptible to failures caused by differential thermal expansion of the joint components. To avoid these complications and to ensure long term reliability, the composite to metal joints in both the support posts and anchor tie bars are effected by shrink fitting the composite tube between an inner metal disc and an outer metal ring. A typical joint configuration is shown in Figure 6.

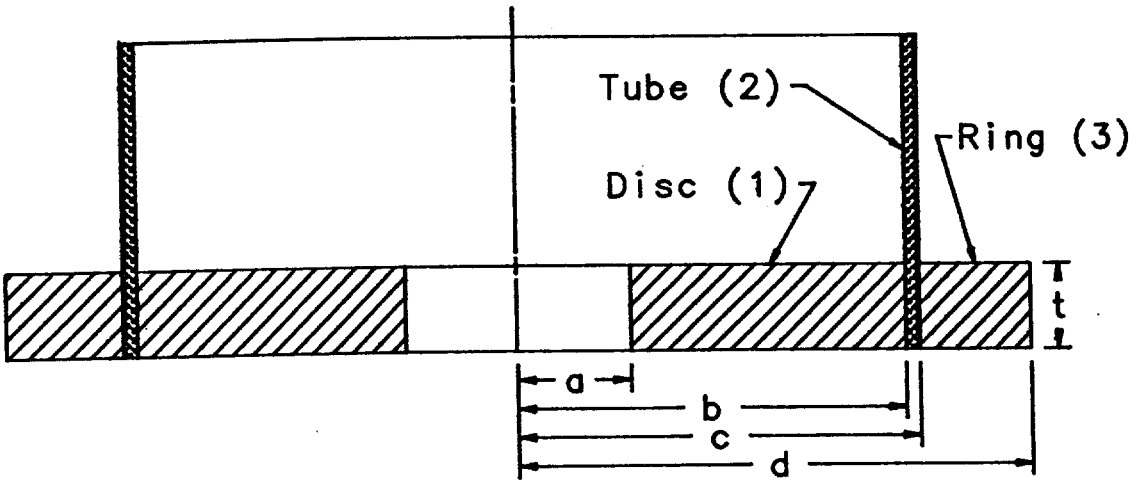

Figure 6. Shrink Fit Joint Notation

Each of the joints in the support posts resists both axial loads and overturning moments. An axial load is one which tries to pull the joint apart. An overturning moment is one which tries to twist it apart. Using the nomenclature in Figure 6 the forces and moments required to cause the joint to fail are given by

$$F_i = P_i(2\pi bt\mu_i) \quad ; \quad F_o = P_o(2\pi ct\mu_o)$$

$$M_i = 4P_i\mu_i b^2 t \quad ; \quad M_o = 4P_o\mu_o c^2 t$$

where F_i, F_o = applied forces which induce slippage of the inner and outer interfaces respectively

M_i, M_o = applied moments which induce slippage of the inner and outer interfaces respectively

μ_i, μ_o = coefficient of friction at the inner and outer interfaces respectively

P_i, P_o = inner and outer interface pressures respectively and are given by

$$P_i = \frac{P_o(k_4+k_5)-\delta_o}{k_6} \quad ; \quad P_o = \frac{\delta_i k_6+\delta_o(k_1+k_2)}{(k_4+k_5)(k_1+k_2)-k_3k_6}$$

where δ_i, δ_o = inner and outer interface radial interference fits respectively

k_1 - k_6 = constant parameters determined by the joint geometry and material properties and are given by

$$k_1 = \frac{b}{E_1}\left(\frac{b^2+a^2}{b^2-a^2}\right) - \nu_1 \quad ; \quad k_2 = \frac{b}{E_2}\left(\frac{c^2+b^2}{c^2-b^2}\right) + \nu_2 \quad ; \quad k_3 = \frac{b}{E_2}\left(\frac{2c^2}{c^2-b^2}\right)$$

$$k_4 = \frac{c}{E_3}\left(\frac{d^2+c^2}{d^2-c^2}\right) + \nu_3 \quad ; \quad k_5 = \frac{c}{E_2}\left(\frac{c^2+b^2}{c^2-b^2}\right) - \nu_2 \quad ; \quad k_6 = \frac{c}{E_2}\left(\frac{2b^2}{c^2-b^2}\right)$$

where E_1, E_2, E_3 = Young's modulus for the disc, tube, and ring respectively

ν_1, ν_2, ν_3 = Poisson's ratio for the disc, tube, and ring respectively

As with the structural and thermal analysis referenced above, a computer program was written which calculates the required radial interferences at the inner and outer interfaces required to produce a joint that satisfies either a maximum input axial force or overturning moment.

Table 3 contains a listing of the analysis results for a typical shrink fit joint. This particular case is for the joint at the 300K end of the support post. The input overturning moment (MRes) for this example was 90000 in-lb. The force to slip (FSlip) was input as zero. The program calculates the interference fit that satisfies the more stringent of these two parameters. The resulting radial interference is 0.0063 inches. The lowermost portion of this listing contains the resulting radial and circumferential stresses (SigR and SigC) in the disc, tube, and ring.

Table 3. Summary of Shrink Fit Analysis

```
*****  Shrink Fit Analysis...Input  *****

Note.....................: Design B - 300K Joint
Dimension, A.....(in):    1.5000
           B.....(in):    3.3918
           C.....(in):    3.5000
           D.....(in):    4.5000
           T.....(in):     .7500
Material property, E1....(psi):  .28E+08
                   V1...........:     .3330
                   E2....(psi):  .20E+07
                   V2...........:     .2000
                   E3....(psi):  .28E+08
                   V3...........:     .3330
Friction coefficient, Mu.....:     .3000
Force to slip, FSlip.....(lb):        .0
Resisting Moment, MRes...(in-lb):  90000.0
```

```
*****  Shrink Fit Analysis...Results  *****

Interference reqd at inner interface...(in):    .0189
                     outer interface...(in):   -.0127

Total radial interference reqd.....(in):    .0063

Contact pressure at inner interface...(psi):  8696.5
                    outer interface...(psi):  8163.3

Actual force to slip.....(lb):  41696.3
       resisting moment.....(in-lb):  90000.0

                                    Ri          Rm          Ro
                                 ========    ========    ========
Inner disc...SigR...(psi):          .0       -8744.3     -8696.5
             SigC...(psi):    -21624.2     -14879.9    -12927.7

Tube.....SigR...(psi):        -8696.5      -8423.6     -8163.3
         SigC...(psi):         8696.5       8423.6      8163.3

Outer ring...SigR...(psi):    -8163.3      -3328.3         .0
             SigC...(psi):    33163.3      28328.3     25000.0
```

Material Selections

References have been made throughout the preceding sections to some of the unique material property issues encountered in this design process. Of particular interest are the composite materials used in the support post and anchor tie bar tubes. Until recently the primary structural composite materials found in superconducting magnets were glass reinforced composites in an epoxy matrix. Familiar names are G-10, G-10CR, G-11, and G-11CR. These continue to be excellent choices. They are readily available, have well characterized structural and thermal properties, are relatively strong, have low thermal conductivity, and are inexpensive.

Recent years have brought developments in new fibers for use in composites, some of which offer advantages in terms of strength, some in terms of thermal conductivity, some in both. It is well known, for example that graphite composites can offer greater strength and stiffness than their glass counterparts. Less known is their low thermal conductivity, particularly at low temperature. Figure 7 is a plot of the thermal conductivity of G-11CR and a uniaxial graphite composite. Note that at room temperature the thermal conductivity of G-11CR is four times less than that of the GRP, however, at approximately 40K the curves cross indicating that at low temperature the GRP may in fact provide greater resistance to conductive heat flow.[5]

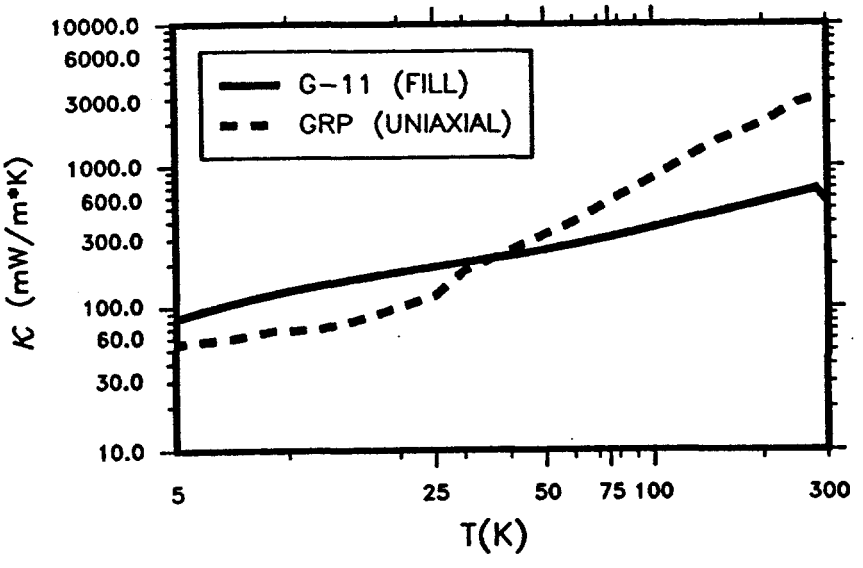

Figure 7. Thermal Conductivity of G-11CR and GRP Tube Material

Table 4. Comparison of Two Structurally Optimized Support Posts

	FRP Outer GRP Inner	FRP Outer FRP Inner
t, outer (inches)	0.109	0.109
t, inner (inches)	0.129	0.201
Q to 80K (W)	2.103	2.038
Q to 20K (W)	0.320	0.370
Q to 4.5K (W)	0.015	0.030

The reentrant design of the support post gave us the option of taking advantage of this behavior. For the outer tube, operating between 300K and 80K, the thermal performance of G-11CR makes it superior to GRP. For the inner tube, operating between 80K and 4.5K, GRP is better.

Table 4 contains the results of the structural optimization described previously and illustrates that the choice of GRP for the inner tube does in fact produce an assembly with lower 4.5K heat load than an assembly which uses G-11CR (FRP) for both tubes.

High strength and low thermal conductivity are not the only considerations for composite materials suitable for use in the support structure. The operating environment, dimensional stability, and fabricability must also be considered. Figure 8 illustrates a sample of a material specification given to potential manufacturers of the composite tubes needed for the suspension system. We have tried to be as specific as necessary without being overly restrictive. The hope being that each manufacturer draw from his own experience in producing a product that meets the needs of the design and which can be mass produced at a reasonable cost.

SSC Composite Tube Specification — T.H.Nicol
Components: Support Post, Inner Tube — 11-20-86 A 01-23-87

Dimension and Direction Notation

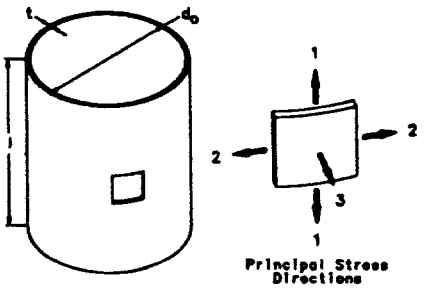

Dimensions
1 (in) : 7.310
d_o (in) : 5.000
t (in) : 0.129

Operating Environment
Temperature Range : 305K → 4.5K
Relative Humidity : 10% → 90%
Pressure Range : Atm → 10^{-6} Torr
Radiation Dosage : 10^8 Rad (20 yrs)

Structural Propeties @ 300K
E_1 (psi) : 10.0 x 10^6 (min)
ν_1 : 0.10→ 03.0
σ_1 (psi) : ±60000 (min,ult)
E_2 (psi) : 10.0 x 10^6 (min)
ν_2 : 0.10 → 03.0
σ_2 (psi) : ±40000 (min, ult)
E_3 (psi) : 5.0 x 10^6 (min)
ν_3 : 0.10 → 0.30
σ_3 (psi) : -30000 (min,ult)

Thermal Conductivity @ 300K
κ_1 (W/cm-K) : 0.0350 (max)
κ_2 (W/cm-K) : 0.0350 (max)
κ_3 (W/cm-K) : nc

Thermal Conductivity @ 77K
κ_1 (W/cm-K) : 0.0067 (max)
κ_2 (W/cm-K) : 0.0067 (max)
κ_3 (W/cm-K) : nc

Thermal Conductivity @ 4.5K
κ_1 (W/cm-K) : 0.0006 (max)
κ_2 (W/cm-K) : 0.0006 (max)
κ_3 (W/cm-K) : nc

Figure 8. Sample Composite Tube Performance Specification

The support posts used in SSC cryostats share vertical and lateral loads induced by shipping, handling, and seismic loads. Thermal contraction of the cold mass assembly during warmup and cooldown necessitates axial sliding between the cold mass and each of the four outboard posts. The center post is attached rigidly to the cold mass assembly to ensure correct axial position within the vacuum vessel. Given no other restraint, this means that the center post would see the entire axial component of any load. A single post is incapable of handling these loads alone. Utilizing a 'strong' post at the center would impose intolerable heat loads on the cryogenic systems.

Ideally one would like an anchor system with negligible thermal impact on the cryogenic systems and which introduced no perturbations into other cryostat components. Recognizing that the bending strength of all five posts could be combined to effectively act as a single axial restraint, we have chosen to connect the 4.5K ring of each post to that of each adjacent post with axial tie bars.

To understand the effectiveness of such a scheme, we must understand the degree to which an axial load applied at the center post is shared by the remaining four posts. Specifically, we need to know the reaction forces at the top of each post, given a force applied at the center. Figure 9 is an equivalent spring diagram of the post and tie bar connections used to determine the stiffness of the total system. Points 1 through 5 represent the tie bar attachment points, point 3 being the top of the center post. The k_p's represent the bending stiffness of each support posts. The k_b's represent the axial stiffness of each tie bar. Grounded points represent the 300K attachment of each post to the cryostat vacuum vessel. The analysis consists of breaking the system into a series of equivalent k's for each post and tie bar connection. These equivalent k's are then used to calculate the total stiffness of the system as shown below.

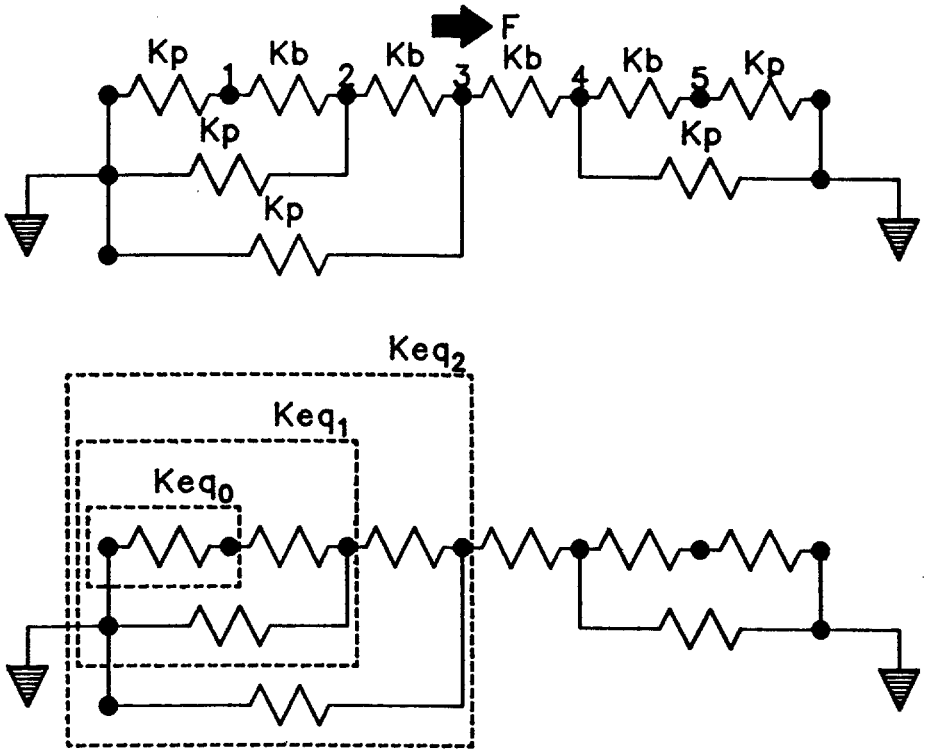

Figure 9. Equivalent Spring Diagram of the Suspension System

$$k_{eq_n} = k_p + \frac{1}{\frac{1}{k_{eq_{n-1}}} + \frac{1}{k_b}} \qquad n = 1..m$$

$$k_{total} = k_p + \frac{2}{\frac{1}{k_{eq_{m-1}}} + \frac{1}{k_b}}$$

where

k_{eq_n} = equivalent stiffnesses for each connection as shown on Figure 9

$k_{eq_0} = k_p$

m = (number of k_b's - 1) / 2

k_{total} = total axial stiffness

For the SSC suspension system

$$m = 2$$

$$k_p \simeq 35000 \text{ lb/in}$$

$$k_b \simeq 200000 \text{ lb/in}$$

resulting in

$$k_{total} \simeq 133000 \text{ lb/in}$$

If the anchor system were 100% efficient the axial stiffness of the complete suspension system would equal 175000 lb/in (35000 lb/in x 5 posts). Given the total stiffness above, the overall anchor efficiency is 76%. Efficiency is defined as the ratio of the actual total stiffness to the sum of the stiffnesses of all five support posts.

Each discrete k_{eq} is used to determine the displacement at the top of each post resulting from the applied force, F. The product of each displacement and k_p yields the reaction force at each post. The load distribution is determined by these individual reactions. Given the above parameters, the center post in an SSC dipole carries 26.4% of the axial component of any induced load. Each of the two posts adjacent to the center carry 19.9% and the outermost two carry 16.9% each.

One final consideration remains in the design of the anchor system and relates to the material selection for the tie bars. Materials commonly selected for use in superconducting magnet cryostats; glass composites, stainless steel, and aluminum, for example, all exhibit decreases in length when cooled from 300K to 4.5K. Selecting such a material for the anchor tie bars would result either in very high tensile loads in the tie bars themselves or very high bending moments in the post assemblies because of the shrinkage which occurs during cooldown. Unlike most materials, however, graphite fibers exhibit a negative coefficient of thermal expansion meaning that they grow when cooled. In most graphite composites this effect is masked by the resin system which shrinks upon cooldown, particularly if the bulk of the fibers are oriented off-axis from the measurement direction.

By pultruding or filament winding graphite fibers with epoxy resin one can create a composite tube with an expansion coefficient from 300K to 4.5K of roughly -0.03% depending on the fiber content and on the fiber and epoxy used. Further, by attaching metal fittings to each end of the tube which shrink upon cooldown one can produce a tube assembly with no net expansion or contraction over the prescribed temperature range. For example, a composite tube 120 inches long, with an expansion coefficient of -0.03% will grow 0.036 inches when cooled from room temperature to 4.5K. Two stainless steel ends, 6 inches long, with an expansion coefficient of 0.3%, shrink 0.018 inches each resulting in a net change in length during cooldown, for the assembly, of zero.

The tie bars used in the present configuration are 120 inches long tubes with an outside diameter of 2 inches and a wall thickness of 0.25 inches. The material is filament wound using graphite fibers in an epoxy matrix. The elastic modulus of the composite is 18×10^6 psi along the axis of the tube. The measured contraction of a complete tie bar when cooled from room temperature to 77K is less than 0.001 inches.

CONCLUDING REMARKS

The suspension system for SSC magnets has evolved toward its current configuration as the result of much analysis and many design iterations, some based on established practice, others developed as complete new concepts. The system described here is a combination of old and new. Support posts in some form have been used for many years, but none, to our knowledge, have been developed into devices which afford such low heat loads and high structural stiffnesses and strengths. Further, none have been developed using shrink fit bonds at all composite to metal joints nor have they played such an integral role in the anchor system performance.

The current suspension system design meets the static structural requirements set forth for SSC magnets and exceeds the required thermal performance at 4.5K. It constitutes an assembly which requires a minimum of added perturbations to other cryostat components and lends itself well to easy fabrication and mass-production. Hopefully it is a design which serves the needs of the SSC and the needs of future applications.

REFERENCES

1. T.H. Nicol et al, A suspension system for superconducting super collider magnets, in: "Proceedings of the Eleventh International Cryogenic Engineering Conference," Butterworths, Surrey, UK (1986).
2. T.H. Nicol et al, SSC magnet cryostat suspension system design, in: "Advances in Cryogenic Engineering" Vol. 33, Plenum Press, New York (1988).
3. SSC Central Design Group, "Superconducting Super Collider Magnet System Requirements," SSC-100, October 1986.
4. R.J. Roark and W.C. Young, "Formulas for Stress and Stain," Fifth Edition, McGraw Hill, New York (1975), p. 428.
5. M. Takeno et al, Thermal and mechanical properties of advanced composite materials at low temperatures, in: "Advances in Cryogenic Engineering" Vol. 32, Plenum Press, New York (1986).